

## Ultraviolet inverse-photoemission and photoemission spectroscopy studies of diluted magnetic semiconductors $\text{Cd}_{1-x}\text{Mn}_x\text{Te}$ ( $0 \leq x \leq 0.7$ )

M. Taniguchi, K. Mimura, H. Sato, J. Harada, K. Miyazaki, and H. Namatame

*Department of Materials Science, Faculty of Science, Hiroshima University, Kagamiyama 1-3, Higashi-Hiroshima 724, Japan*

Y. Ueda

*Tokuyama National College of Technology, Kume-Takajo 3538, Tokuyama 745, Japan*

(Received 25 April 1994; revised manuscript received 16 August 1994)

Electronic structures of  $\text{Cd}_{1-x}\text{Mn}_x\text{Te}$  films ( $0 \leq x \leq 0.7$ ) grown epitaxially on GaAs(100) substrates have been investigated by means of *in situ* measurements of conduction-band inverse-photoemission and valence-band photoemission spectra. With increasing Mn concentration, the energy position of the conduction-band minimum shifts almost linearly toward higher energy relative to the valence-band maximum (VBM) as a result of an increasing contribution of the higher-lying Mn 4s level relative to the Cd 5s level. Features observed at 3.6 and  $-3.4$  eV relative to the VBM are ascribed to emission from the Mn  $3d\downarrow$  and  $3d\uparrow$  states with  $e_g$  symmetry, respectively, providing a spin-exchange splitting energy of  $7.0 \pm 0.2$  eV. This value compares well with the predicted value in the theoretical investigation of electronic structures and magnetic properties of  $\text{Cd}_{1-x}\text{Mn}_x\text{Te}$ . Apart from one-electron band theory, the whole spectrum including multielectron satellites in the energy region between  $-5$  and  $-9$  eV is found to be in good agreement with that calculated in terms of the configuration-interaction theory using a  $\text{Mn}^{2+}(\text{Te}^{2-})_4$  model cluster.

### I. INTRODUCTION

Mn-substituted II-VI diluted magnetic semiconductors (DMS's) have attracted a great deal of attention as a new class of semiconductors, since the replacement of the cations in the II-VI semiconductors yields unusual magneto-transport and magneto-optical properties.<sup>1,2</sup> Such phenomena stem from the *sp*-band-Mn  $3d$  and Mn-Mn exchange interactions through the hybridization between the *sp* band and Mn  $3d$  states.

The band structure and magnetic properties of Mn-substituted DMS's have been theoretically investigated<sup>3-13</sup> based on a local-spin-density-augmented-spherical-wave method,<sup>3,4</sup> a combination of *ab initio* spin-polarized band calculations, a semiempirical tight-binding model containing available experimental data, and consideration of alloying effects,<sup>5-8</sup> self-consistent spin-polarized spin-density-functional band-structure calculations,<sup>9</sup> spin-polarized, self-consistent local-spin-density total-energy and band-structure calculations,<sup>10,11</sup> and self-consistent local-density pseudofunction theory.<sup>12,13</sup> The theoretical *sp*-band-Mn  $3d$  and Mn-Mn exchange constants<sup>5-8</sup> are in fairly good agreement with results from the enhanced Zeeman splittings of free-exciton lines in magneto-optical experiments,<sup>14</sup> and those from magnetization<sup>15,16</sup> and neutron-scattering<sup>17</sup> experiments, respectively.

An attempt to investigate directly the conduction-band states of  $\text{Cd}_{1-x}\text{Mn}_x\text{Te}$  has been made by Franciosi and co-workers using bremsstrahlung isochromat spectroscopy (BIS) at a photon energy of 1486.6 eV with a spectrometer resolution of 0.7 eV.<sup>12,13</sup> The Mn-derived feature was observed at 4.8 eV above the valence-band maximum (VBM), and a Mn  $3d$  spin-exchange splitting

energy ( $U_{\text{eff}}$ ) was estimated to be  $8.3 \pm 0.4$  eV. From comparison with electronic structures of antiferromagnetic zinc-blende MnTe based on a local-density-functional model calculation,<sup>12,13</sup> the authors claimed that the ground-state configuration of the Mn is primarily  $(d\uparrow)^5(s\uparrow)(p\uparrow)$  rather than  $(d\uparrow)^5s^2$ . The BIS measurements, however, suffered from experimental difficulties such as electron-beam-induced sample damage and a serious electrostatic charging effect.<sup>18</sup> Unoccupied states of  $\text{Cd}_{0.5}\text{Mn}_{0.5}\text{Te}$  have been also investigated by Kisiel *et al.* using x-ray-absorption near-edge structure (XANES) spectroscopy.<sup>19</sup> The Te  $L_1$ - and  $L_3$ -edge XANES spectra were analyzed in combination with the electronic structure calculation in terms of a localized muffin-tin orbital method with a local-spin-density approximation. The best agreement between the experiment and theory was obtained in the case for which the Mn  $3d$  states were placed approximately at  $3.3 \pm 0.5$  eV above the VBM.

In recent years, the contribution of Mn  $3d$  states to the valence-band density of states (DOS) has been investigated experimentally to study the hybridization between the *sp*-band and Mn  $3d$  states.<sup>12,13,20-24</sup> Resonant photoemission experiments using tunable synchrotron radiation (SR) successfully revealed a measure of the Mn  $3d$  partial DOS of  $\text{Cd}_{1-x}\text{Mn}_x\text{Te}$  with a Mn concentration ( $x$ ) of 0.65.<sup>21</sup> The spectral features have been analyzed in terms of a configuration-interaction (CI) calculation using a  $\text{Mn}^{2+}(\text{Te}^{2-})_4$  model cluster.<sup>21,22</sup> The Mn  $3d$  photoemission spectrum has also been reproduced on the basis of the Anderson impurity model with parameters by *ab initio* calculations, including the multiplet effect.<sup>25</sup> Very recently, the electronic structures of substitutional  $3d$  transition-metal impurities in II-VI semiconductors have been investigated by means of the CI calculation using

cluster and Anderson impurity models.<sup>26</sup> The Mn 3*d* photoemission<sup>21,22</sup> and inverse-photoemission<sup>12</sup> spectra, *d-d\** optical-absorption spectra,<sup>27</sup> *sp*-band-Mn 3*d* exchange constants,<sup>28</sup> and donor and acceptor ionization energies<sup>29</sup> were calculated with the same set of parameters.<sup>26</sup> These theoretical investigations for Cd<sub>1-x</sub>Mn<sub>x</sub>Te (Refs. 21, 22, 25, and 26) confirm a significant Mn 3*d*-Te 5*p* hybridization which allows for sufficient screening of the 3*d* excitations by the ligand to *d*-hole charge transfer in the valence bands. In that sense, the spectral density at the top 5 eV of the valence bands can be assumed to be a good approximation for a measure of the valence-band DOS.<sup>21</sup>

In this paper, we present conduction- and valence-band spectra of Cd<sub>1-x</sub>Mn<sub>x</sub>Te films ( $0 \leq x \leq 0.7$ ) grown epitaxially on GaAs(100) substrates, measured *in situ* by means of ultraviolet inverse-photoemission and photoemission spectroscopies (IPES and UPS). The IPES spectra have been successfully obtained by preparing thin epitaxial films on GaAs(100) substrates with very low resistivity to overcome the difficulty on the electrostatic charging effect. *In situ* measurements of IPES and UPS spectra realize a connection between these spectra at the Fermi level,<sup>30</sup> and make it possible to determine directly that the  $U_{\text{eff}}$  value is  $7.0 \pm 0.2$  eV. We shall discuss the IPES and UPS spectra in comparison with the results of the band-structure calculation in terms of the tight-binding semiempirical coherent potential approximation for Cd<sub>1-x</sub>Mn<sub>x</sub>Te,<sup>5</sup> and also with those of the CI calculation using a Mn<sup>2+</sup>(Te<sup>2-</sup>)<sub>4</sub> model cluster<sup>26</sup> in distinction from the one-electron band picture.

## II. EXPERIMENT

The IPES spectrometer<sup>31,32</sup> used in the present experiments consists of a low-energy electron gun of the Erdman-Zipf type with an energy spread of 0.25 eV, an Al reflection mirror coated with a MgF<sub>2</sub> film, and a bandpass photon detector with a full width at half maximum of 0.47 eV and a maximum response at 9.43 eV. All components are mounted in an ultrahigh-vacuum chamber under a base pressure below  $7 \times 10^{-11}$  Torr. The overall energy resolution of the spectrometer was 0.56 eV. The electron beam was injected normal to the sample surfaces.

The UPS spectrometer connected with the IPES apparatus is composed of a He discharge lamp ( $\hbar\omega = 21.2$  eV) and a double-stage cylindrical-mirror analyzer to obtain angle-integrated spectra. The energy resolution was set at 0.2 eV. The working pressure of the UPS chamber was  $3 \times 10^{-9}$  Torr under the operation of the discharge lamp, though the base pressure was  $4 \times 10^{-10}$  Torr. Energy positions of the Fermi level in the IPES and UPS spectra were experimentally determined using spectra for a fresh film of polycrystalline Au.<sup>32</sup> IPES and UPS spectra measured *in situ* on the same sample surface were connected at the Fermi level.

All measurements of IPES and UPS spectra were carried out at room temperature. The energy was referred to a VBM determined by extrapolating the steep leading edge of the highest valence-band peak to the baseline.

Samples used for IPES and UPS experiments were Cd<sub>1-x</sub>Mn<sub>x</sub>Te films ( $x = 0, 0.2, 0.3, 0.5,$  and  $0.7$ ) grown by the hot wall epitaxy (HWE) technique on (100)-oriented Si-doped *n*-type GaAs substrates with a misorientation of 2° toward the next [110] direction,<sup>33</sup> and with an impurity concentration of  $1.0\text{--}2.5 \times 10^{18}$  cm<sup>-3</sup> or a resistivity of  $1.5\text{--}2.8 \times 10^{-3}$  Ω cm. The HWE reactor consists of a CdTe furnace with an additional Te source for compensation of the vacancies and the Mn furnace. A flip-flop method<sup>34</sup> was employed to obtain various thicknesses and *x*'s of the films. The thickness was controlled by a repetition number of the flip-flop motion, and *x* by periods during the stay of the substrate over the CdTe and Mn furnaces, which were operated at 520 and 860 °C, respectively.

Prior to the crystal growth, the substrates were chemically etched in a 5:1:1 solution of H<sub>2</sub>SO<sub>4</sub>:H<sub>2</sub>O<sub>2</sub>:H<sub>2</sub>O. The substrate loaded into a vacuum chamber was heated at 580 °C for 2 min to remove the oxide layer. During the growth, the substrate was kept constant at 300 °C, and the pressure was  $1\text{--}5 \times 10^{-8}$  Torr under the operation of the CdTe and Mn furnaces. After the growth of the film, the vacuum chamber was immediately evacuated into the middle of  $10^{-9}$  Torr, keeping the substrate temperature above 250 °C, and the sample was transferred into the UPS chamber. In this way, a clean surface of the Cd<sub>1-x</sub>Mn<sub>x</sub>Te epitaxial film was successfully obtained. The crystal orientation and *x* value of the epitaxial film with a thickness of 0.5–1 μm were checked by x-ray diffraction.<sup>35</sup>

The IPES spectra are much more sensitive to an electrostatic charging effect in comparison with the UPS spectra.<sup>36</sup> To avoid such an effect, the thickness of film was reduced by decreasing only the repetition number of the flip-flop motion without changing any other parameters in the growth condition for the thick Cd<sub>1-x</sub>Mn<sub>x</sub>Te(100) film, until the IPES spectrum exhibited no electrostatic charging effect. The thickness of the samples used for the IPES and UPS experiments was measured using a surface profiler (high precision optical stylus surface measuring instrument, Kosaka Ltd.). The typical value of the thickness was about 30 nm.

In general, CdTe epitaxial films can grow on GaAs(100) substrates with (100) and (111) orientations, depending on the growth conditions,<sup>37</sup> and often mixed films are obtained. In the present experiments, it is reasonably assumed that thin films used for the IPES and UPS measurements would be (100)-oriented films, because Cd<sub>1-x</sub>Mn<sub>x</sub>Te epitaxial films with (100) orientation grew steadily under suitable parameters mentioned above. The UPS spectra for thin Cd<sub>1-x</sub>Mn<sub>x</sub>Te films, which exhibited no electrostatic charging effect in the IPES measurements, were fully consistent with those for the thick Cd<sub>1-x</sub>Mn<sub>x</sub>Te(100) films. The UPS spectra for thick Cd<sub>1-x</sub>Mn<sub>x</sub>Te(100) films with enough thickness for a determination of the orientation using x-ray diffraction were free from the electrostatic charging effect, and consistent with those for bulk alloys.

Residual strain is known to be important and to affect, for example, the band-gap energy of CdTe. The amount of the strain-induced change in the band-gap energy is,

however, estimated to be  $\sim 10$  meV,<sup>38,39</sup> and is negligible in comparison with the energy resolution of 0.56 and 0.2 eV in the IPES and UPS measurements, respectively.

The  $x$  values of the thin epitaxial films were again evaluated by x-ray photoemission spectroscopy (XPS; ESCA 5400, Perkin Elmer) using integrated emission intensities of the Cd  $3d$ , Mn  $2p$ , and Te  $3d$  core levels of the epitaxial films, after IPES and UPS measurements. The XPS spectra for the bulk  $\text{Cd}_{1-x}\text{Mn}_x\text{Te}$  specimens were used as a reference. The  $x$  values evaluated by XPS measurements for thin epitaxial films were in good agreement with those for thick films estimated from x-ray diffraction within  $x = \pm 0.05$ .

Close attention was paid to reliable ohmic contacts, which were alloyed onto the back surface of the substrate using Sn to avoid an uncontrolled voltage drop at the GaAs substrate–Mo sheet interface. The Mo sheet was used to prevent a reaction between the GaAs substrate and the CuBe sample holder during a heating process at 580°C for 2 min.

### III. RESULTS AND DISCUSSION

Figure 1 shows a series of conduction-band IPES and valence-band UPS spectra of  $\text{Cd}_{1-x}\text{Mn}_x\text{Te}$  films grown epitaxially on GaAs(100) substrates with values of  $x$  of 0, 0.2, 0.3, 0.5, and 0.7. The IPES spectrum of pure CdTe exhibits peak structures at 3.7, 5.4, 6.4, and 9.0 eV above the VBM (vertical bars). From comparison with the results of a band-structure calculation based on the nonlocal semiempirical pseudopotential method of Chelikowsky and Cohen,<sup>40</sup> the first peak at 3.7 eV is attributed to the DOS feature due to flat regions of conduction bands around the  $X_6$  and  $X_7$  symmetry points. The weak

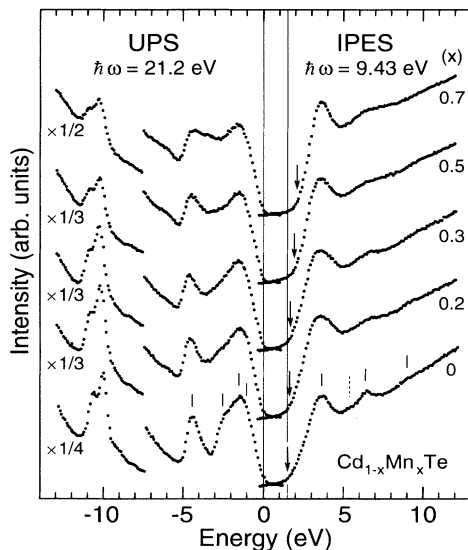


FIG. 1. A series of the conduction-band IPES and valence-band UPS spectra of  $\text{Cd}_{1-x}\text{Mn}_x\text{Te}$  films grown epitaxially on GaAs(100) substrates with  $x = 0, 0.2, 0.3, 0.5,$  and  $0.7$ . Intensities of the IPES and UPS spectra are tentatively normalized at 12 and  $-1.5$  eV, respectively. Vertical bars indicate the positions of structures, and arrows indicate the thresholds of the IPES spectra. Energies are referred to the VBM.

second peak at 5.4 eV, the third one at 6.4 eV, and the fourth one at 9.0 eV are ascribed to those around the  $\Gamma_7$  and  $\Gamma_8, L_{4,5}$  and  $L_6$ , and  $\Lambda$  symmetry points, respectively.

As regards the energy positions of structures, the spectrum is quantitatively consistent with the ultraviolet IPES spectrum for the CdTe(110) cleaved surface measured at normal incidence using the tunable-photon mode,<sup>41</sup> except for the surface-resonance peak on CdTe(110) at 2.8 eV above the VBM.<sup>42</sup> On the basis of the band-structure calculation of Chadi *et al.*,<sup>43</sup> features observed at 3.7 and 6.4 eV above the VBM were attributed to the  $X_6$  and  $\Gamma_8$  symmetry points of the conduction bands, respectively.<sup>41</sup> A BIS spectrum at a photon energy of 1486.6 eV on the CdTe(110) cleaved surface has been also reported, emphasizing structures at 4.1, 6.7, 9.6, 11.3, 12.5, and 15 eV above the VBM.<sup>44</sup> From a comparison with results of a nonlocal semiempirical-pseudopotential calculation,<sup>40</sup> peaks at 4.1 and 6.7 eV were ascribed to the DOS feature of conduction bands originating from states around the  $\Delta$  and  $X$  symmetry points, and that derived from states in low-symmetry directions of the Brillouin zone,<sup>44</sup> respectively. We find that peak structures at 4.1, 6.7, and 9.6 eV in the BIS spectrum correspond to those at 3.7, 6.4, and 9.0 eV in the present IPES spectrum, respectively, after a shift of the peaks in the BIS spectrum by 0.3–0.6 eV toward lower energy.

The energy position of the conduction-band minimum (CBM) can be roughly evaluated by extrapolating the leading edge of the lowest conduction-band peak to the baseline. One notices the threshold energy of the IPES spectrum of CdTe to be 1.5 eV, in good agreement with the direct-band-gap energy of 1.53 eV. With an increase of  $x$ , the threshold shifts almost linearly toward higher energy, as shown by the vertical arrows in Fig. 1. At  $x = 0.7$ , the spectral rise at the threshold and the width of the main peak become steep and narrow, respectively, while the energy of the main peak remains almost unchanged at 3.6 eV. In addition, the main peak is assumed to exhibit a slight increase in intensity with  $x$ , if the spectra of  $\text{Cd}_{1-x}\text{Mn}_x\text{Te}$  ( $0.2 \leq x \leq 0.7$ ) are tentatively normalized to the intensity at 12 eV (Ref. 45) in the spectrum of pure CdTe. The energy of the narrow main peak is almost independent of the incidence angle of the electron beam.

The higher-energy shift of the threshold with  $x$  is consistent with the variation of the fundamental band-gap energy determined by optical-absorption<sup>46</sup> and ellipsometry measurements,<sup>47</sup> and can be understood as a result of an increasing contribution of the higher-lying Mn  $4s$  level relative to the Cd  $5s$  level.<sup>5,46,47</sup> The amount of the shift at  $x = 0.7$  is, however, smaller by about 0.2 eV than that obtained from experiments on interband transitions,<sup>46,47</sup> mainly due to the characteristics of the overall energy resolution of the IPES spectrometer.<sup>48</sup>

The narrowing, constant energy position and a slight increase in intensity of the main peak with  $x$  suggest Mn-derived states with fairly localized character at 3.6 eV above the VBM. The energy position is in agreement with  $3.3 \pm 0.5$  eV predicted for the Mn  $3d \downarrow$  states from

the analysis of the Te  $L_1$  and  $L_3$  XANES spectra.<sup>19</sup> A constant energy of the narrow main peak for the incidence angle of the electron beam is also consistent with the localized character.

On the other hand, the UPS spectrum of pure CdTe has previously been reported by several authors and discussed in detail. We recall here that the features at  $-1.0$ ,  $-1.5$ ,  $-2.5$ , and  $-4.4$  eV (vertical bars) reflect maxima in the DOS of valence bands derived mainly from flat regions around the  $L_3$ ,  $X_5$ ,  $W_2$ - $\Sigma_1^{\text{min}}$ , and  $L_1$  symmetry points, respectively.<sup>49,50</sup> The valence-band DOS is primarily composed of Te  $5p$  states. Increasing  $x$  from 0 to 0.3, we find no discernible change in the shape of the valence bands, except for a slight blurring of fine structures. For  $x$  above 0.5, however, additional emission shows up clearly between the two prominent peaks at  $-1.5$  and  $-4.4$  eV. Shapes of the UPS spectra are consistent with those for  $\text{Cd}_{1-x}\text{Mn}_x\text{Te}$  ( $0 \leq x \leq 0.65$ ) measured at an excitation-photon energy of 22 eV by means of SR photoemission.<sup>20</sup> An increasing spectral density between  $-1.5$  and  $-4.4$  eV with  $x$  is predominantly due to Mn  $3d$  emission, with a main peak at  $-3.4$  eV.<sup>20,21</sup> Although the positions of the Cd  $4d$  core levels have been reported to be almost independent of  $x$  in an earlier experiment,<sup>20</sup> energies of  $4d_{5/2}$  and  $4d_{3/2}$  relative to the VBM are found to shift almost linearly from  $-10.10$  and  $-10.75$  eV ( $x=0$ ) to  $-10.30$  and  $-10.95$  eV ( $x=0.7$ ), respectively, in the present study.<sup>51</sup> The origin of these energy shifts is discussed below, in terms of the band-structure calculation.<sup>5</sup>

While the Mn  $3d$  features in the UPS spectra are clearly observed as an increase in intensity at  $-3.4$  eV with  $x$ , those in the IPES spectra can be recognized only in the form of a narrowing of the main peak at a constant energy of 3.6 eV, and as a slight increase in intensity of the main peak under the tentative normalization of the spectra. We assume that the following would be main reasons why the Mn  $3d$  features are less pronounced in the IPES spectra in comparison with those in the UPS spectra in Fig. 1: (1) The photoabsorption cross section of the Mn  $3d$  states<sup>52</sup> at 9.43 eV (IPES) is smaller by a factor of 3 than that at 21.2 eV (UPS). (2) The Mn  $3d$  features in the IPES spectra show up at an energy just overlapping with the first peak in the spectrum of CdTe, whereas those in the UPS spectra appear at an energy between the two prominent DOS peaks.

Figure 2(a) shows the conduction-band IPES and valence-band UPS spectra of  $\text{Cd}_{0.3}\text{Mn}_{0.7}\text{Te}$  and CdTe films. The valence-band photoemission spectrum of  $\text{Cd}_{0.4}\text{Mn}_{0.6}\text{Te}$  measured at an excitation-photon energy of 49.5 eV (on resonance) is also shown to demonstrate the Mn  $3d$  emission.<sup>53</sup> One again notices a main peak at 3.6 eV and a broad and weak structure around 6.5 eV in the IPES spectrum, a valence-band structure between 0 and  $-2.5$  eV, a main peak at  $-3.4$  eV in the UPS spectrum, and a broad satellite between  $-5$  and  $-9$  eV in the spectrum measured at 49.5 eV.

First we compare Fig. 2(a) with the theoretical total and Mn  $3d$  partial DOS's of  $\text{Cd}_{0.4}\text{Mn}_{0.6}\text{Te}$  calculated by Ehrenreich *et al.*<sup>5</sup> in Fig. 2(b). The total DOS of CdTe is also shown in Fig. 2(c) for the convenience of discussion.

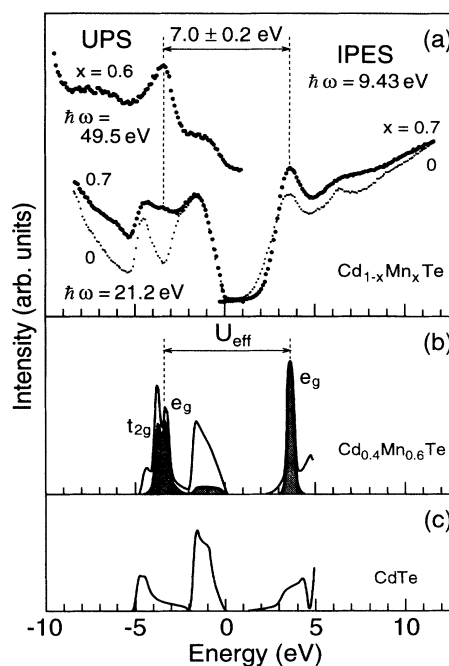


FIG. 2. (a) Conduction-band IPES and valence-band UPS spectra of  $\text{Cd}_{0.3}\text{Mn}_{0.7}\text{Te}$  and CdTe films. To demonstrate the Mn  $3d$  emission, the valence-band spectrum of  $\text{Cd}_{0.4}\text{Mn}_{0.6}\text{Te}$  measured at 49.5 eV (on resonance) is also shown. (b) Total and Mn  $3d$  partial (shaded area) DOS's of  $\text{Cd}_{0.4}\text{Mn}_{0.6}\text{Te}$  and (c) total DOS of CdTe based on tight-binding calculations (Ref. 5).

The zero energy in the theoretical DOS's is referred to the VBM of CdTe. In Fig. 2(b), a prominent DOS peak due to the unoccupied Mn  $3d\downarrow$  states with  $e_g$  symmetry is placed at 3.6 eV. The energy position of this peak is coincident with that of the first DOS peak of CdTe. On the other hand, the occupied Mn  $3d\uparrow$  states split into two peaks as a result of  $sp$ - $d$  hybridization. The lower states with  $t_{2g}$  symmetry hybridize more strongly than the higher states with  $e_g$  symmetry in the tetrahedral environment, and shift to lower energy due to a repulsion from the upper Te  $5p$  valence bands. The corresponding  $3d$  admixture in the upper valence-band region is responsible for the Mn  $3d$  DOS in the energy region between 0 and  $-2$  eV and the slight shift of the VBM toward higher energy. Such a shift of the VBM is, in fact, observed in a form of an increase in energy separations between the VBM and Cd  $4d$  core levels in Fig. 1.

The  $U_{\text{eff}}$  value, the energy necessary to add one  $3d$  electron to a  $\text{Mn}^{2+}$  ion,<sup>5-8</sup> is taken to be 7.0 eV. The connections between the electronic structure in Fig. 2(b) and the  $sp$ -band-Mn  $3d$  and Mn-Mn exchange interactions have been extensively investigated.<sup>6,7</sup> In particular, the Mn-Mn exchange constant has been calculated quantitatively and shown to result primarily from hybridization-induced antiferromagnetic superexchange. Then authors developed a physically transparent model of both the  $sp$ -band-Mn  $3d$  and Mn-Mn exchange using only four parameters: the valence-band-edge energy  $E_v$ , the energy of occupied Mn  $3d$  states  $E_d$ , the  $p$ - $d$  hybridi-

zation parameter  $V_{pd}$ , and  $U_{\text{eff}}$ . For numerical results, the principal uncertainty lies mainly in the parameters of  $V_{pd}$ , and  $U_{\text{eff}}$ .<sup>6</sup>

One notices that the Mn-derived features in the IPES and UPS spectra in Fig. 2(a) are in good agreement with those in the calculated DOS curves. Taking into account the experimental features observed for the narrow main peak at 3.6 eV in the IPES spectrum as well as the comparison between the experiment and theory in Fig. 2, we assign the peak at 3.6 eV to the Mn 3d $\downarrow$  states, and evaluate the  $U_{\text{eff}}$  value to be  $7.0 \pm 0.2$  eV from Fig. 2(a). The splitting energy of  $7.0 \pm 0.2$  eV is in quantitative agreement with the predicted  $U_{\text{eff}}$  value, and supports the electronic structure model for the estimation of the nearest-neighbor Mn-Mn exchange constant ( $J^{dd}$ ) of  $\text{Cd}_{1-x}\text{Mn}_x\text{Te}$ , using input parameters such as  $E_v - E_d = 3.4$  eV taken from photoemission experiments,<sup>20,21</sup>  $U_{\text{eff}} = 7.0$  eV,  $V_{pd} = 0.219$  eV estimated from the experimental  $sp$ - $d$  exchange constant,<sup>54</sup> and the Mn-Te bond length of 2.759 Å determined by extended x-ray-absorption fine-structure experiments.<sup>55</sup> Authors further calculated a chemical trend of  $J^{dd}$  in  $\text{Cd}_{1-x}\text{Mn}_x\text{Y}$  ( $Y = \text{Te, Se, S}$ ). The predicted increase in  $J^{dd}$  from telluride to selenide is in reasonable agreement with the increase observed experimentally. The larger predicted increase in  $J^{dd}$  from selenide to sulfide overestimates the experimental trend, which may be corrected when more accurate input parameters become available.

Recent first-principles calculations for  $\text{Cd}_{1-x}\text{Mn}_x\text{Te}$  by Wei and Zunger predicted a  $U_{\text{eff}}$  of 4.9 eV.<sup>10,11</sup> Calculations for paramagnetic zinc-blende MnTe by Masek, Velicky, and Janis provided a value of 5.5 eV,<sup>56</sup> and those for antiferromagnetic zinc-blende MnTe by Podgórny suggested a value of about 4 eV for the splitting energy.<sup>9</sup> All calculated values are substantially smaller than our experimental value of  $7.0 \pm 0.2$  eV.<sup>57</sup> On the other hand, the earlier experimental value determined from the BIS measurements is  $8.3 \pm 0.4$  eV,<sup>12</sup> and substantially larger than the present value. For this discrepancy, it should be noted that the photoemission and BIS measurements were made for different cleaved surfaces of  $\text{Cd}_{0.8}\text{Mn}_{0.2}\text{Te}$  alloy,<sup>12</sup> though the position of the Fermi level in the band gap depends significantly on the cleaved faces of crystals. *In situ* measurements of the IPES and UPS spectra in the present study rule out such an irreversible shift of the Fermi level.

With respect to the Mn-derived feature at 4.6 eV in the reflectivity<sup>58</sup> and ellipsometry<sup>47</sup> measurements of  $\text{Cd}_{1-x}\text{Mn}_x\text{Te}$ , Kendelewicz tentatively interpreted the structure as coming from interband transitions from the  $sp$  valence band to the unoccupied Mn 3d states.<sup>58</sup> The initial states were related to the maximum in the valence-band DOS at 1.8 eV below the VBM: the states around the  $X_5$  symmetry point. This places the unoccupied Mn 3d states at 2.8 eV above the VBM. On the other hand, Franciosi *et al.* attributed the structure to optical transition from the top of the  $sp$  valence-band states to the unoccupied Mn 3d states at  $4.8 \pm 0.3$  eV above the VBM on the basis of their experimental result.<sup>12</sup> Both values of 2.8 and 4.8 eV are in rather poor agreement

with the present result of 3.6 eV.

The location of the unoccupied Mn 3d states at 3.6 eV above the VBM in the present study provides a plausible interpretation. We remember that the valence-band spectrum of pure CdTe exhibits a DOS structure at  $-1.0$  eV, which is primarily derived from the flat region of valence bands around the  $L_3$  symmetry point. In addition, the shape of the  $sp$  part of the valence-band spectrum does not change appreciably when Mn is added.<sup>20</sup> The location of the unoccupied Mn 3d states at 3.6 eV above the VBM in the present study thus suggests that the optical transition at 4.6 eV is most probably due to transitions from the states around the  $L_3$  symmetry point at  $-1.0$  eV to the unoccupied Mn 3d states, in agreement with the assignment by Larson *et al.*<sup>6</sup>

In spite of the good correspondence between the experiment and energy-band theory, the theory cannot interpret the multielectron satellite in the energy region between  $-5$  and  $-9$  eV. Nor can it explain the intratomic  $d$ - $d^*$  optical absorption observed at about 2.2 eV for  $\text{Cd}_{1-x}\text{Mn}_x\text{Te}$  with  $x \geq 0.4$ .<sup>27</sup> Gunnarsson, Postni-

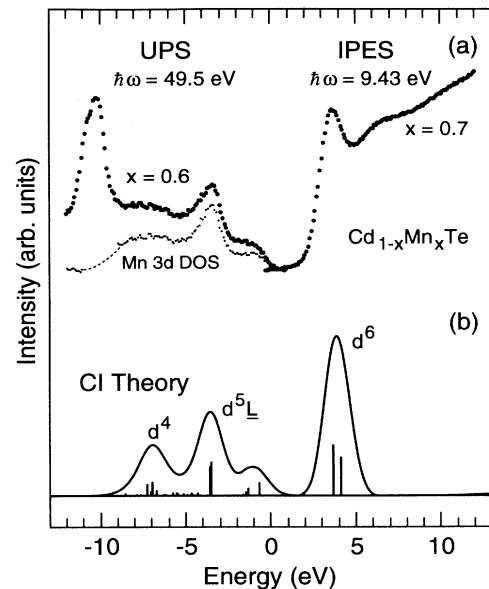


FIG. 3. (a) Conduction-band IPES spectrum of  $\text{Cd}_{0.3}\text{Mn}_{0.7}\text{Te}$  film, valence-band photoemission spectrum of  $\text{Cd}_{0.4}\text{Mn}_{0.6}\text{Te}$  measured at 49.5 eV (on resonance), and a measure of the Mn 3d partial DOS evaluated from resonant photoemission experiment in the Mn 3p-3d core excitation region (dotted curves). (b) Mn 3d-derived photoemission spectra of  $\text{Cd}_{1-x}\text{Mn}_x\text{Te}$  calculated on the basis of the configuration-interaction theory (Ref. 26). In the calculation,  $d^5$ ,  $d^6\bar{L}$ ,  $d^7\bar{L}^2$  and  $d^4$ ,  $d^5\bar{L}$ ,  $d^6\bar{L}^2$  configurations are taken into account for the initial and final states, respectively, where  $\bar{L}$  represents a ligand hole. The line spectra are calculated using parameters of  $U = 4.0$  eV,  $\Delta = 2.0$  eV, and  $(pd\sigma) = -1.1$  eV. Here  $U$  is Coulomb correlation energy of the Mn 3d electrons, and  $\Delta$  is the ligand-to-metal charge-transfer energy. In addition,  $(pd\sigma)$  represents a  $p$ - $d$  transfer integral and  $(pd\sigma)/(pd\pi)$  is fixed at  $-2.16$ . The solid curves are constructed by a convolution of the line spectra, with Gaussian and Lorentzian functions for the sake of comparison.

kov, and Anderson presented the results of *ab initio* calculations for parameters in the Anderson model, such as the energy-dependent *p-d* hybridization parameters and a Mn *3d* Coulomb correlation energy of 7.3 eV.<sup>25</sup> Without any empirical parameters, the Mn *3d* photoemission spectrum was fairly well reproduced including the multielectron satellites.

Very recently, Mizokawa and Fujimori calculated the Mn *3d*-derived inverse-photoemission and photoemission spectra of  $\text{Cd}_{1-x}\text{Mn}_x\text{Te}$  in terms of the CI theory.<sup>26</sup> Figure 3 exhibits (a) the conduction-band IPES spectrum of  $\text{Cd}_{0.3}\text{Mn}_{0.7}\text{Te}$  film, valence-band photoemission spectrum of  $\text{Cd}_{0.4}\text{Mn}_{0.6}\text{Te}$  measured at 49.5 eV (on resonance), and a measure of the Mn *3d* partial DOS evaluated from resonant photoemission experiments in the Mn *3p-3d* core excitation region<sup>53</sup> (dotted curves), and (b) the calculated spectra (solid curves).<sup>26</sup> CI analysis revealed that the feature between 0 and  $-5$  eV with a main peak at  $-3.4$  eV is predominantly due to transitions into the  $d^5\bar{L}$  final states, whereas the satellite between  $-5$  and  $-9$  eV is ascribed to transitions into the  $d^4$  final states. Here the  $\bar{L}$  denotes a ligand hole. On the same line of argument, the main peak at 3.6 eV in the Mn *3d* inverse-photoemission spectrum is attributed to transitions into the  $d^6$  final states.

Previous analysis for the Mn *3d* partial DOS of  $\text{Cd}_{1-x}\text{Mn}_x\text{Te}$  provided a Mn *3d* Coulomb correlation energy of 7.5 eV (Refs. 21 and 22) [ $U \equiv E(3d^4) + E(3d^6) - 2E(3d^5)$ , where  $E(3d^n)$  is the center of gravity of the  $3d^n$  multiplet], different from the value of 4.0 eV in Ref. 26. The discrepancy in  $U$  originates mainly from the fact that the relevant optical and magnetic properties and impurity states have been interpreted consistently using the same set of parameters.<sup>59</sup> In addition, the previous analysis was performed using only the  $d^5$ ,  $d^6\bar{L}$  and  $d^4$ ,  $d^5\bar{L}$  configurations as the initial and final states, respectively, while recent analysis takes further account of the  $d^7\bar{L}^2$  and  $d^6\bar{L}^2$  configurations for the initial and final states. The inclusion of the  $d^7\bar{L}^2$  and  $d^6\bar{L}^2$  configurations has an influence upon the number and energy positions of the structures in the spectra.

#### IV. CONCLUSIONS

We have measured the conduction-band IPES and valence-band UPS spectra of  $\text{Cd}_{1-x}\text{Mn}_x\text{Te}$  films ( $0 \leq x \leq 0.7$ ) grown epitaxially on GaAs(100) substrates. The IPES spectrum of pure CdTe shows peak structures at 3.7, 5.4, 6.4, and 9.0 eV above the VBM. On the basis of the results of band-structure calculation,<sup>40</sup> these structures are interpreted to be associated with the DOS features due to particular flat regions of conduction bands around the  $X_6$  and  $X_7$ ,  $\Gamma_7$  and  $\Gamma_8$ ,  $L_{4,5}$  and  $L_6$ , and  $\Lambda$  symmetry points, respectively. With increasing  $x$ , the energy position of the CBM relative to the VBM shifts linearly toward higher energy as a result of an increasing

contribution of the Mn *4s* states to the conduction bands.

The energy position of the Mn *3d*  $\downarrow$  states at 3.6 eV above the VBM in the present study is in good agreement with that predicted from the analysis of the Te  $L_1$  and  $L_3$  edge XANES spectra combined with the electronic structure calculation.<sup>19</sup> The  $U_{\text{eff}}$  value is directly estimated to be  $7.0 \pm 0.2$  eV. This value compares well with the predicted spin-exchange splitting energy of 7.0 eV in support of the electronic structure model,<sup>5-8</sup> though the present result is substantially smaller than the earlier experimental value of  $8.3 \pm 0.4$  eV from the photoemission and BIS measurements.<sup>12</sup>

For the initial states of transitions responsible for the Mn-derived feature at 4.6 eV in the reflectivity spectra,<sup>58</sup> the valence-band states around the  $X_5$  symmetry points are assumed to be the most probable candidates based on the location of the Mn *3d*  $\downarrow$  states at 3.6 eV.

Aside from the energy-band theory, the peak at 3.6 eV, features between 0 and  $-5$  eV with a main peak at  $-3.4$  eV, and those between  $-5$  and  $-9$  eV are assigned to the  $d^6$ ,  $d^5\bar{L}$ , and  $d^4$  final states, respectively, on the basis of CI calculations using cluster<sup>26</sup> and Anderson impurity<sup>25,26</sup> models.

*In situ* measurements of IPES and UPS spectra of  $\text{Zn}_{1-x}\text{Mn}_x\text{Te}$  films ( $0 \leq x \leq 0.7$ ) grown epitaxially on GaAs(100) substrates by the HWE technique have recently been made.<sup>60</sup> The IPES spectrum of pure ZnTe exhibits peak structures at 4.0 and 6.8 eV above the VBM, reflecting DOS maxima of the *sp* conduction bands. With the increase of  $x$ , a Mn-derived feature shows up clearly at 3.5 eV, namely 0.5 eV below the first peak in the spectrum of ZnTe. Peaks at 3.5 and  $-3.7$  eV (Ref. 23) in the IPES and UPS spectra have been ascribed to emission from the Mn *3d*  $\downarrow$  and *3d*  $\uparrow$  states with  $e_g$  symmetry, respectively. In spite of the difference in band structure between ZnTe and CdTe, the  $U_{\text{eff}}$  of  $7.2 \pm 0.2$  eV evaluated for  $\text{Zn}_{1-x}\text{Mn}_x\text{Te}$  is very close to  $7.0 \pm 0.2$  eV in the present study for  $\text{Cd}_{1-x}\text{Mn}_x\text{Te}$ , implying the intra-atomic nature of the  $U_{\text{eff}}$ .

#### ACKNOWLEDGMENTS

The authors are grateful to Professor T. Oguchi for stimulating discussions on theoretical aspects, to Professor S. Miyazaki and Dr. M. Ohashi for measurements of thickness and XPS spectra of epitaxial films, and to A. Minami for an electron-probe microanalysis of bulk specimens, respectively. We thank also the staff of SRL-ISSP for the operation of SOR-RING and technical support. This work is partly supported by the Grant-in-Aid for Scientific Research from the Ministry of Education, Science and Culture, Japan, Iketani Science and Technology Foundation, The Ogasawara Foundation for The Promotion of Science and Technology, The Murata Science Foundation, and Shimazu Science Foundation.

<sup>1</sup>*Diluted Magnetic Semiconductors*, edited by J. K. Furdyna and J. Kossut, Semiconductors and Semimetals Vol. 25 (Academic, New York, 1988), and references therein.

<sup>2</sup>*Diluted Magnetic Semiconductors*, edited by M. Jain (World

Scientific, Singapore, 1991), and references therein.

<sup>3</sup>B. E. Larson, K. C. Hass, H. Ehrenreich, and A. E. Carlsson, *Solid State Commun.* **56**, 347 (1985).

<sup>4</sup>K. C. Hass, B. E. Larson, H. Ehrenreich, and A. E. Carlsson, J.

- Magn. Mater. **54-57**, 1283 (1986).
- <sup>5</sup>H. Ehrenreich, K. C. Hass, N. F. Johnson, B. E. Larson, and R. J. Lampert, in *Proceedings of the 18th International Conference of the Physics of Semiconductors*, edited by O. Engstrom (World Scientific, Singapore, 1987), pp. 1751–1754.
- <sup>6</sup>B. E. Larson, K. C. Hass, H. Ehrenreich, and A. E. Carlsson, Phys. Rev. B **37**, 4137 (1988).
- <sup>7</sup>B. E. Larson and H. Ehrenreich, Phys. Rev. B **39**, 1747 (1989).
- <sup>8</sup>B. E. Larson and H. Ehrenreich, J. Appl. Phys. **67**, 5084 (1990).
- <sup>9</sup>M. Podgórný, Z. Phys. B **69**, 501 (1988).
- <sup>10</sup>S.-H. Wei and A. Zunger, Phys. Rev. Lett. **56**, 2391 (1986).
- <sup>11</sup>S.-H. Wei and A. Zunger, Phys. Rev. B **35**, 2340 (1987).
- <sup>12</sup>A. Franciosi, A. Wall, Y. Gao, J. H. Weaver, M.-H. Tsai, J. D. Dow, R. V. Kasowski, R. Reifenberger, and F. Pool, Phys. Rev. B **40**, 12 009 (1989).
- <sup>13</sup>A. Wall, A. Franciosi, Y. Gao, J. H. Weaver, M.-H. Tsai, J. D. Dow, and R. V. Kasowski, J. Vac. Sci. Technol. A **7**, 656 (1989).
- <sup>14</sup>J. A. Gaj, R. Planel, and G. Fishman, Solid State Commun. **29**, 435 (1979).
- <sup>15</sup>B. E. Larson, K. C. Hass, and R. L. Aggwal, Phys. Rev. B **33**, 1789 (1986).
- <sup>16</sup>Y. Shapira and N. F. Olivera, Jr., Phys. Rev. B **35**, 6888 (1987).
- <sup>17</sup>T. Giebultowicz, B. Lebech, B. Buras, W. Minor, H. Kepa, and R. R. Galazka, J. Appl. Phys. **55**, 2305 (1984).
- <sup>18</sup>The spectra were obtained as the sum of 20 quantitatively consistent spectra from different cleavage surfaces, which corresponds to a total of some 150 h of data integration with a primary electron beam current of about 200  $\mu\text{A}$ .
- <sup>19</sup>A. Kisiel, J. Oleszkiewicz, M. Podgórný, G. Dalba, F. Rocca, and E. Burattini, J. Cryst. Growth **101**, 239 (1990).
- <sup>20</sup>M. Taniguchi, L. Ley, R. L. Johnson, J. Ghijsen, and M. Cardona, Phys. Rev. B **33**, 1206 (1986).
- <sup>21</sup>L. Ley, M. Taniguchi, J. Ghijsen, R. L. Johnson, and A. Fujimori, Phys. Rev. B **35**, 2839 (1987).
- <sup>22</sup>M. Taniguchi, A. Fujimori, M. Fujisawa, T. Mori, I. Souma, and Y. Oka, Solid State Commun. **62**, 431 (1987).
- <sup>23</sup>M. Taniguchi, K. Soda, I. Souma, and Y. Oka, Phys. Rev. B **46**, 15 789 (1992).
- <sup>24</sup>A. Wall, A. Raisanen, G. Haugstad, L. Vanzetti, and A. Franciosi, Phys. Rev. B **44**, 8185 (1991).
- <sup>25</sup>O. Gunnarsson, A. V. Postnikov, and O. K. Andersen, Phys. Rev. B **39**, 1708 (1989); **40**, 10 407 (1989).
- <sup>26</sup>T. Mizokawa and A. Fujimori, Phys. Rev. B **48**, 14 150 (1993); A. Fujimori and T. Mizokawa, in *II-VI Semiconductor Compounds*, edited by M. Jain (World Scientific, Singapore, 1992), p. 103.
- <sup>27</sup>Y. R. Lee and A. K. Ramdas, Solid State Commun. **51**, 861 (1984).
- <sup>28</sup>J. K. Furdyna, J. Appl. Phys. **64**, R29 (1988).
- <sup>29</sup>A. Fazzio, M. J. Caldas, and A. Zunger, Phys. Rev. B **30**, 3430 (1984).
- <sup>30</sup>The position of the Fermi level in the band gaps of semiconductors depends significantly upon respective samples, while energies of IPES and UPS spectra can be defined experimentally with respect to the Fermi level. Connection of the IPES and UPS spectra at the Fermi level by means of *in situ* measurements is essentially important to evaluate accurately the energy separation between the peak in the IPES spectrum and that in the UPS spectrum.
- <sup>31</sup>K. Yokoyama, K. Nishihara, K. Mimura, Y. Hari, M. Taniguchi, Y. Ueda, and M. Fujisawa, Rev. Sci. Instrum. **64**, 87 (1993).
- <sup>32</sup>Y. Ueda, K. Nishihara, K. Mimura, Y. Hari, M. Taniguchi, and M. Fujisawa, Nucl. Instrum. Methods A **330**, 140 (1993).
- <sup>33</sup>H. Sitter, K. Lischka, W. Faschinger, J. Wolfrum, H. Pascher, and J. L. Pautrat, J. Cryst. Growth **86**, 377 (1988).
- <sup>34</sup>H. Fujiyasu, A. Ishida, H. Kuwabara, S. Shimomura, S. Takaoka, and K. Murase, Surf. Sci. **142**, 579 (1984); K. Suzuki, M. Nakamura, I. Souma, K. Yanata, Y. Oka, and H. Fujiyasu, J. Cryst. Growth **117**, 881 (1992). In the flip-flop motion, the GaAs substrate moves from one HWE furnace to the other.
- <sup>35</sup>N. Bottka, J. Stankiewicz, and W. Gariat, J. Appl. Phys. **52**, 4189 (1981).
- <sup>36</sup>All bulk samples with  $x \geq 0.2$  prepared by a Bridgmann method had high resistivity in the range of  $10^6$ – $10^8 \Omega$ . The IPES spectra exhibited the electrostatic charging effect for all of these samples, even for an incident-electron beam of 1  $\mu\text{A}$ , while the UPS spectra were free from such an effect.
- <sup>37</sup>K. Lischka, E. J. Fantner, T. W. Ryan, and H. Sitter, Appl. Phys. Lett. **55**, 1309 (1989).
- <sup>38</sup>J. H. Lee, S. B. Kim, B. J. Koo, I. H. Chung, M. Jung, H. L. Park, and T. W. Kim, Solid State Commun. **84**, 901 (1992).
- <sup>39</sup>H. Tatsuoka, H. Kuwabara, Y. Nakanishi, and H. Fujiyasu, J. Appl. Phys. **67**, 6860 (1990).
- <sup>40</sup>J. R. Cherkowsky and M. L. Cohen, Phys. Rev. B **14**, 556 (1976).
- <sup>41</sup>K. O. Magnusson, U. O. Karlsson, D. Straub, S. A. Flodstrom, and F. J. Himpsel, Phys. Rev. B **36**, 6566 (1987).
- <sup>42</sup>We have also observed the surface resonance peak on CdTe(110), in agreement with the result in Ref. 41. Then In-doped CdTe single crystals with very low resistivity were especially used to avoid charging effect. After scraping the CdTe(110) surface with a diamond file, the surface-resonance peak disappeared, while the other bulk structures remain almost unchanged.
- <sup>43</sup>D. Chadi, J. P. Walter, M. L. Cohen, Y. Petroff, and M. Balkanski, Phys. Rev. B **5**, 3058 (1972).
- <sup>44</sup>A. Wall, Y. Gao, A. Raisanen, A. Franciosi, and J. R. Cherkowsky, Phys. Rev. B **43**, 4988 (1991).
- <sup>45</sup>Comparison of intensities among the IPES spectra of  $\text{Cd}_{1-x}\text{Mn}_x\text{Te}$  could be made tentatively under the assumption that the intensities in the high-energy region well above the CBM are independent of  $x$ , as employed in Ref. 12. In the present experiment, intensities of the IPES spectra have been compared after the normalization at various energies between 12 and 15 eV, providing no significant change in the trend for the  $x$  dependence of relative intensities. To our knowledge, no evaluations of the absolute intensity of the IPES spectrum or relative intensities among a series of the IPES spectra have been reported so far, due mainly to experimental difficulties, though a method for the background subtraction is in progress [K. W. Goodman and V. E. Henrich, Phys. Rev. B **49**, 4827 (1994)].
- <sup>46</sup>N. T. Khoi and J. A. Gaj, Phys. Status Solidi B **83**, K133 (1977); K. C. Hass and H. Ehrenreich, J. Vac. Sci. Technol. A **1**, 1678 (1983).
- <sup>47</sup>P. Lautenschlager, S. Logothetidis, L. Vina, and M. Cardona, Phys. Rev. B **32**, 3811 (1985), and references therein.
- <sup>48</sup>The characteristic curve has an asymmetric feature extending toward lower energy with a full width at half maximum of 0.56 eV (Ref. 32). Spectral broadening due to such an instrumental resolution is significant for measurements of the intense and steep edges.
- <sup>49</sup>L. Ley, A. Pollak, F. R. McFeely, S. P. Kowalczyk, and D. A. Shirley, Phys. Rev. B **9**, 600 (1974).

- <sup>50</sup>N. J. Shevchik, J. Tejada, and M. Cardona, *Phys. Rev. B* **9**, 2627 (1974).
- <sup>51</sup>In addition to the case of the  $\text{Cd}_{1-x}\text{Mn}_x\text{Te}$  films, we have found that energies of the Cd  $4d$  core levels in bulk  $\text{Cd}_{1-x}\text{Mn}_x\text{Te}$  alloys also shift almost linearly with  $x$  relative to the VBM. The discrepancy between present and earlier results could be due to the accuracy of the determination of the VBM. In earlier experiments, excitation-photon energies above 50 eV were used to measure the valence-band and core-level spectra, including the Te  $4d_{5/2}$  and  $4d_{3/2}$  core levels at  $-39.3$  and  $-40.7$  eV relative to the VBM, respectively, in contrast to the present experiments with an excitation light of 21.2 eV. DOS's in the vicinity of the VBM are composed mainly of Te  $5p$  states. The position of the VBM could be determined with higher accuracy in the present experiment compared to the earlier one, since the photoabsorption cross section of the Te  $5p$  states at 21.2 eV is about one order of magnitude larger than that at 50 eV (Ref. 52). The scraping for samples with high resistivity (Ref. 20) sometimes cause a blurring of the threshold and peak structures.
- <sup>52</sup>J. J. Yeh and I. Lindau, *At. Data Nucl. Data Tables* **32**, 45 (1985); **32**, 72 (1985).
- <sup>53</sup>N. Happo, H. Sato, K. Mimura, S. Hosokawa, M. Taniguchi, Y. Ueda, and M. Koyama, *Phys. Rev. B* **50**, 12211 (1994). The on-resonance spectra for  $x \geq \sim 0.4$  are reasonably assumed to demonstrate the Mn  $3d$  emission, since the cross section of the Mn  $3d$  states at 49.5 eV is about 30 times larger than that of the Te  $5p$  states (Ref. 52).
- <sup>54</sup>D. Heiman, Y. Shapira, and S. Foner, *Solid State Commun.* **51**, 603 (1984).
- <sup>55</sup>A. Balzarotti, M. Czyżyk, A. Kisiel, N. Motta, M. Podgórný, and M. Zimnal-Starnawska, *Phys. Rev. B* **30**, 2295 (1984); A. Balzarotti, N. Motta, A. Kisiel, M. Zimnal-Starnawska, M. T. Czyżyk, and M. Podgórný, *ibid.* **31**, 7526 (1985).
- <sup>56</sup>J. Masek, B. Velicky, and V. Janis, *Acta Phys. Pol. A* **69**, 1107 (1986).
- <sup>57</sup>Our  $U_{\text{eff}}$  value of  $7.0 \pm 0.2$  eV compares well with that of 6.8 eV estimated from the local-density functional calculations after correction of the  $sp$  band gap to the experimental value (Ref. 12), though the raw splitting energy before the correction is not available.
- <sup>58</sup>T. Kendelewicz, *J. Phys. C* **14**, L407 (1981).
- <sup>59</sup>The Mn  $3d$  photoemission spectrum of  $\text{Cd}_{1-x}\text{Mn}_x\text{Te}$  in Ref. 22 was reproduced with  $U = 7.5$  eV,  $\epsilon_d - \epsilon_p + U = 3.5$  eV, and  $(pd\pi) = 0.47$  eV.  $\epsilon_d - \epsilon_p + U$  and  $(pd\pi)$  are equal to  $\Delta$  and  $-(pd\sigma)/2.16$ , respectively, in Ref. 26. The spectral shape of the Mn  $3d$  partial DOS is determined predominantly by  $\Delta - U$ , and can be reproduced to some extent using either the parameter of  $\Delta - U$  in Ref. 22 or that in Ref. 26, except for an effect of the inclusion of additional  $d^7\bar{L}^2$  and  $d^6\bar{L}^2$  configurations in Ref. 26. When the  $d - d^*$  optical absorption, Mn  $3d$  inverse photoemission, and photoemission spectra are interpreted consistently using the same set of parameters, a reduction of  $\Delta$  is required. This reduction of  $\Delta$  leads mainly to the reduction of  $U$  from 7.5 to 4.0 eV [T. Mizokawa (private communication)].
- <sup>60</sup>M. Taniguchi, N. Happo, K. Mimura, H. Sato, J. Harada, K. Miyazaki, H. Namatame, and Y. Ueda (unpublished).